Published in final edited form as:
Anal Chem. 2008 May 1; 80(9): 3182–3189. doi:10.1021/ac702367m.

Fast Electrophoretic Separation Optimization Using Gradient Micro Free-Flow Electrophoresis

Bryan R. Fonslow and **Michael T. Bowser***
University of Minnesota, Department of Chemistry, 207 Pleasant Street SE, Minneapolis, Minnesota 55455

Abstract

The continuous nature of micro free-flow electrophoresis (μ-FFE) was used to monitor the effect of a gradient of buffer conditions on the separation. This unique application has great potential for fast optimization of separation conditions and estimation of equilibrium constants. COMSOL was used to model pressure profiles in the development of a new μ-FFE design that allowed even application of a buffer gradient across the separation channel. The new design was fabricated in an all glass device using our previously published multiple-depth etch method (Fonslow, B. R.; Barocas, V. H.; Bowser, M. T. *Anal. Chem.* 2006, *78*, 5369–5374, [ref 1]). Fluorescein solutions were used to characterize the applied gradients in the separation channel. Linear gradients were observed when buffer conditions were varied over a period of 5–10 min. The effect of a gradient of 0–50 mM hydroxypropyl-β-cyclodextrin (HP-β-CD) on the separation of a group of 4-fluoro-7-nitro-2,1,3-benzoxadiazole (NBD-F) labeled primary amines was monitored as a proof of concept experiment. Direct comparisons to capillary electrophoresis (CE) separations performed under the same conditions were made. Gradient μ-FFE recorded 60 separations during a 5 min gradient allowing nearly complete coverage across a range of HP-β-CD concentrations. In comparison, 4 h were required to assess 15 sets of conditions across the same range of HP-β-CD concentrations using CE. Qualitatively, μ-FFE separations were predictive of the migration order and spacing of peaks in CE electropherograms measured under the same conditions. Data were fit to equations describing 1:1 analyte–additive binding to allow a more quantitative comparison between gradient μ-FFE and CE.

Micro free-flow electrophoresis (μ-FFE) is an analytical separation technique used to separate a continuously flowing stream of charged analytes.[2,3] A thin sample stream is introduced into a planar separation channel with buffer running in parallel. An electric field is applied perpendicularly across the separation channel, and charged analytes are deflected laterally based on their electrophoretic mobility. Thus far, μ-FFE separations have been limited to simple separations of fluorescent dyes,[4–6] fluorescently labeled amino acids,[2] and fluorescently labeled proteins.[3,7] μ-FFE's larger-scale, preparative counterpart has proven useful in separating a range of analytes, including cells,[8,9] cellular components,[10–14] and proteins.[15–17] In the near future, μ-FFE could be useful in analysis or micropreparative separations of the same analytes.

Recently several researchers have investigated a variety of fabrication methods for μ-FFE devices to improve their performance.[4–6,18–20] In early designs two major problems were encountered. Inefficient removal of electrolysis products, manifested as bubbles, from the electrode channels degraded separations.[4] Also, channel designs used to minimize the effects of the bubbles reduced the electric field applied in the separation channel.[5,6] These problems have since been surmounted using methods such as a two-depth channel design[1] and capacitive

* To whom correspondence should be addressed. E-mail: bowser@umn.edu. Phone: (612) 624-0873. Fax: (612) 626-7541.

electrodes.[21] With multiple working μ-FFE designs, experiments with these microfluidic chips has now moved on to separation optimization.[22] Studies were performed to understand the dominant band broadening and separation mechanisms in μ-FFE. As a result, general strategies for optimizing basic parameters such as flow rate and voltage were developed. Although this simplifies optimization of instrumental settings for separations using μ-FFE, the need for a strategy for optimizing chemical variables remains.

Electrophoretic separations can be optimized by changing multiple variables important to the separation mechanism. For comigrating or poorly resolved peaks, changing the separation conditions can allow for resolution of the analyte peaks. Some of the conditions specific to electrophoretic separations that can be varied include buffer composition, ionic strength, pH, additives, and channel wall coatings.[23] Therefore, there are many variables that can be changed to optimize a separation, requiring many separations at many different conditions to be performed until an optimum is reached. In traditional separations this can quickly become a time-consuming process. Additionally, only a discrete number of conditions are usually tested, opening the possibility of missing a local optimum set of conditions.

The continuous nature of μ-FFE separations offers an alternative approach. Because the pressure-driven flow is orthogonal to the electrophoretic separation, the ability to change the buffer conditions while monitoring the resulting change in electrophoretic separation is possible. Testing a range of conditions is therefore as simple as monitoring the separation while varying the composition of the separation buffer over a short period of time. In the current manuscript, we demonstrate the effect of a simple gradient of cyclodextrin concentration on the separation of a group of fluorescently labeled amino acids. Additionally, key design aspects of the μ-FFE device necessary for proper application of the buffer gradient are discussed.

Experimental Section

Reagents and Chemicals

Unless otherwise noted, all chemicals were purchased from Sigma-Aldrich (St. Louis, MO). Deionized (DI) water (18.2 MΩ, Millipore, Billerica, MA) was used for all preparations unless otherwise noted. Separation buffer consisted of 25 mM HEPES, adjusted to pH = 6.50 using 1 M NaOH and filtered through a 0.2 μm membrane filter (Fisher Scientific, Fairlawn, NJ). Hydroxypropyl-β-cyclodextrin (HP-β-CD, Cargill, Cedar Rapids, IA) was dissolved in separation buffer at a concentration of 50 mM. A stock solution of poly(vinyl alcohol) (PVA, 98–99% hydrolyzed, average MW 31 000–50 000) at 5% w/w was dissolved in DI water at 90 °C for 1 h with stirring. Stock solutions of glycine, L-serine, and phosphorylethanolamine (PEA) were prepared in DI water at ~20 mM. The primary amines were diluted to ~1 mM in the reaction buffer of 100 mM borate (Mallinckrodt, Paris, KY) and 25 mM HP-β-CD at pH 10.5 to a total volume of 450 μL. The fluorogenic reaction was performed by adding 50 μL of 4-fluoro-7-nitro-2,1,3-benzoxadiazole (NBD-F, TCI-Ace, Portland, OR) in 50:50 methanol (Mallinckrodt) and 50 μM HCl (Mallinckrodt) to the reaction mixture to a final concentration of ~10 mM, then heated for 5 min at 60 °C. Piranha solutions (4:1 H_2SO_4–H_2O_2, Ashland Chemical, Dublin, OH) were used to clean glass wafers and etch deposited Ti. Aqua regia (3:1 HCl–HNO_3, Ashland Chemical) was used to etch the Pt. Concentrated HF (Ashland Chemical) was used to etch the glass wafers. Silver conductive epoxy (MG Chemicals, Surrey, BC, Canada) was used to make electrical connections to the chip.

Chip Fabrication

A two-step etch method to create a multiple depth μ-FFE device was used as previously described[1] with the new design shown in Figure 1. Briefly, standard photolithography techniques were used to etch 52 μm deep electrode channels into a 1.1 mm borofloat wafer

(Precision Glass & Optics, Santa Ana, CA). A second photolithography step was used to etch the remaining channels. The final depths of the electrode and remaining channels were 71 and 19 μm, respectively. Titanium (100 nm) and platinum (150 nm) layers were deposited followed by a third photolithography procedure to define the electrodes in the side channels. A second wafer, predrilled with access holes and deposited with a ~90 nm thick layer of amorphous silicon (a-Si), was aligned with the etched, electrode-deposited wafer, and 900 V was applied for 2 h at 450 °C and 5 μbar to anodically bond the two wafers. Nanoports (Upchurch Scientific, Oak Harbor, WA) were attached to the access holes using manufacturer's procedures. Electrodes were connected to the wires using silver conductive epoxy. The chip was perfused with 1 M NaOH until the channels were clear (180 min) to remove unwanted a-Si. Channel walls were coated with 0.05% w/w PVA using Gilges' method[24] by pumping at 3 mL/ min for 15 min.

Fluid Modeling and Channel Design

Computational modeling of the fluid flow in the μ-FFE devices was performed using the steady-state diffusion analysis module within the commercially available finite element method software, COMSOL (version 3.3, COMSOL, Inc., Burlington, MA). μ-FFE designs were drawn in 2-D (see Figure 2) using the CAD environment in COMSOL. Modeling the pressure profiles within different channel designs was possible using the diffusion model due to the similarity of equations for concentration based on diffusion (eq 1) and pressure based on linear velocity (eq 2) where D is a diffusion coefficient, c is concentration, v is linear velocity, and P is pressure.

$$\nabla \cdot (-D\nabla c) = 0 \tag{1}$$

$$\nabla \cdot (-\upsilon \nabla P) = 0 \tag{2}$$

Subdomains, i.e., channels of differing depths, were spatially defined as solids and numerically expressed as diffusion coefficients using the ratio of linear velocities determined by theory.[1] Boundary conditions defined outlets (P = 0), inlets (P = 1), and channel walls (insulation/ symmetry) of the μ-FFE designs numerically. A mesh was generated using the default normal mesh size. After the problem was solved, the data was postprocessed as a contour plot with 100 levels. Iterative geometrical changes to the channel design were made until the pressure profile was flat and perpendicular to the direction of flow in the separation channel as shown in Figure 2B.

μ-FFE Separations and Buffer Additive Gradient Generation

Separation buffer was pumped into the buffer inlet at 0.5 mL/min (0.16 cm/s in the separation channel) from two syringes connected by a mixing tee as shown in Figure 1. Mixing occurred as solution traveled from the mixing tee to the μ-FFE inlet in a 40 cm length of 0.03 in i.d." Teflon tubing (Upchurch Scientific). NBD-labeled primary amines were pumped into the sample channel at 0.1 μL/min (0.25 cm/s in sample channel). A separation voltage of 225 V (214 V/cm) was applied at the right electrode with the left electrode held at ground. The buffer additive gradient was generated using the setup shown in Figure 1. One syringe pump (Pump 22, Harvard Apparatus, Holliston, MA) pumped separation buffer into the mixing tee while the other pumped buffer containing the additive. A home-written LabView 7.0 program (National Instruments, Austin, TX) was used to vary the flow rates of the individual syringe pumps, while keeping the total flow rate constant. Deionized water and 100 μM fluorescein

were used in place of the separation buffer and additive, respectively, in experiments to characterize the gradient.

μ-FFE Instrumentation, Data Collection, and Processing

A SMZ 1500 stereomicroscope (Nikon Corp., Tokyo, Japan) mounted with a 100 W X-Cite fiber-optic metal halide lamp (Nikon Corp.) and Cascade 512B CCD camera (Photometrics, Tucson, AZ) was used for fluorescence imaging. Analyte detection was performed using the 0.75× zoom to image the 1 cm wide separation channel 2 cm downstream from the sample inlet. For laser-induced fluorescence (LIF) detection, a 150 mW Ar^+ laser (Melles Griot, Carlsbad, CA) was expanded to a ~2.5 cm wide by ~150 *μm* thick line across the separation channel of the chip directly below the microscope objective. The microscope was equipped with an Endow GFP bandpass emission filter cube (Nikon Corp) containing two bandpass filters (450–490 nm and 500–550 nm) and a dichroic mirror (495 nm cutoff). A 1.6× objective was used for collection with a 0.7× CCD camera lens. MetaVue software (Downington, PA) was used for image collection and processing. During fluorescein gradient tests, images were acquired every 15 s (5 min gradient) and every 30 s (10 and 20 min gradient) with an exposure time of 100 ms. During gradient separations, images were acquired every 5 s for 6.25 min using an exposure time of 1 s with 4095 intensifier gain. Analysis of linescans across the analyte streams (analogous to electropherograms) was performed using Cutter 5.0.[25]

CE Separations and Viscosity Measurements

Separations were performed on a P/ACE MDQ capillary electrophoresis system (Beckman-Coulter, Fullerton, CA) using a 50 *μ*m i.d./360 *μ*m o.d. capillary (Polymicro Technologies, Pheonix, AZ) cut to 32 cm (20.2 cm to detector). The capillary was conditioned once prior to use with 1 M NaOH for 10 min at 20 psi, separation buffer for 5 min at 20 psi, then 5 min at 30 kV. Varying concentrations of HP-*β*-CD in the separation buffer were prepared by mixing appropriate volumes of separation buffer with buffer containing 50 mM HP-*β*-CD. Sample was injected at 0.1 psi for 5 s, and separations were performed at 30 kV. The capillary was rinsed between separations at 20 psi for 1 min with methanol, then separation buffer. Detection was performed using laser-induced fluorescence with a 488 nm Ar^+ laser and 520 nm bandpass filter at 4 Hz. Viscosity measurements were made using the method described by Peng[26] by injecting the sample and pressure rinsing at 10 psi until the injected peak was detected. The ratio of the elution times of the analyte peaks during the pressure rinses at varying HP-*β*-CD concentrations were used to determine the viscosity correction factor as shown in the following equation:

$$\nu = \frac{t_{\text{HP}-\beta-\text{CD}}}{t_0} \tag{3}$$

where ν is the viscosity correction, $t_{\text{HP-}\beta\text{-CD}}$ is the elution time at varying HP-*β*-CD concentrations, and t_0 is the elution time without HP-*β*-CD. From these results the following relationship between ν and [HP-*β*-CD] was found:

$$\nu = 3.15\ \text{M}^{-1}\left[\text{HP}-\beta-\text{CD}\right] + 0.9973 \tag{4}$$

Equation 4 was used to calculate the viscosity correction factor ν at all HP-*β*-CD concentrations used to estimate equilibrium constants with *μ*-FFE and CE.

Equilibrium Constant Estimation

Dissociation constants of the analyte–HP-β-CD complexes were estimated using the mobility shift of a given analyte induced by the interaction with the changing HP-β-CD concentration. A nonlinear regression assuming single-site binding was used to fit the mobility shift data according to the following equation:[26]

$$\nu\mu_{EP} - \mu_0 = \frac{(\mu_{EP,AC} - \mu_0)}{K_D + [HP-\beta-CD]} \quad (5)$$

where μ_{EP} is the viscosity corrected electrophoretic mobility at varying HP-β-CD concentrations, μ_0 is the electrophoretic mobility of the uncomplexed analyte, $\mu_{EP,AC}$ is the mobility of the analyte–HP-β-CD complex, K_D is the dissociation constant, and [HP-β-CD] is the HP-β-CD concentration. For CE results, μ_{EP} and μ_0 were found by subtracting the mobility of the electroosmotic flow marker from the apparent total mobility of analytes. μ_0 was subtracted from all mobilities before fitting to eq 5. For μ-FFE results, μ_0 was found by averaging the mobilities from images acquired prior to application of the gradient (1 min 15 s, 15 images). μ_0 was again subtracted from all other mobilities and set to zero before fitting to eq 5. A sixth-order polynomial was used to fit the fluorescein gradient data and then used to estimate the HP-β-CD concentrations. Viscosity corrections for CE and μ-FFE were made at the different HP-β-CD concentrations by multiplying the electrophoretic mobility by the viscosity correction factor (ν). The viscosity data could not be obtained during μ-FFE separations, so eq 4 was used to calculate the viscosity correction factor across the range of HP-β-CD concentrations.

Results and Discussion

μ-FFE Design for Gradient Applications

Preliminary experiments using fluorescein gradients were attempted using our earlier μ-FFE design[1] shown in Figure 2A. These experiments clearly showed that this design was not appropriate for gradient experiments. Instead of observing a single gradient across the separation channel, three separate gradients were detected: one on the left side of the separation channel, one in the middle, and one on the right. Each separate gradient was generated by one of the three buffer inlets of the chip. Despite previous particle velocimetry experiments that indicated defined linear velocity regions based on channel depth,[1] fluorescein gradient experiments clearly demonstrated buffer entering the separation channel from the electrode channel. This is problematic because the linear velocity in the electrode channels is ~16 times higher than that in the separation channel. The gradient therefore increased faster at the edges of the separation channel than in the middle. This phenomenon was confirmed using COMSOL and is illustrated in Figure 2A. As described in the methods section, COMSOL was used to model the pressure gradient through the device. Arrows were drawn perpendicular to the equal pressure lines to demonstrate the flow trajectory out of the electrode channels into the separation channel.

An additional problem was introduced by the three separate buffer inlets used in our earlier μ-FFE design.[1] The time for the gradient to travel from the mixing cross to each of these inlets needed to be balanced precisely so that the gradient was applied across the top of the chip evenly. This was not straightforward because the linear velocity through the electrode channels was ~16 times that through separation channel. The linear velocity in the channels dictated the flow rate through the connective tubing, making precise balancing of connective tubing residence times difficult.

The most obvious solution for ensuring an even application of the gradient and equalizing separation channel and electrode channel pressures was to create a single buffer inlet for the μ-FFE device. As shown in Figure 2B, flow splitting to the different depth channels was performed on-chip, minimizing any time discrepancies from linear velocity differences. After multiple iterations, the design shown in Figure 2B was found to give the flattest pressure profiles in the separation channel while isolating electrode channel flow from separation channel flow, as shown by the flow trajectories depicted by the arrows. Two key features made these results possible: (1) One buffer inlet feeds the electrode and separation channels. A single buffer inlet guarantees equal pressures across the top of the electrode and separation channels. In this case, different depth channels are analogous to parallel resistors so the pressure drop should be equal along the length of the channel. Channel depth does not affect pressure but instead determines the fluid linear velocity.[1] With the flow path lengths equal, the flows will be completely parallel and thus isolated. (2) Two triangles make up the top of the separation channel. Because of the large diamond shape necessary to incorporate a sample channel into the device, two triangles define the top of the separation channel. The near equidistance from the tip of the triangle to the base allows for nearly equal pressure drop because it is directly proportional to length. Although slightly curved, the pressure profile at the inlet of the sample is nearly flat and flattens further shortly down the separation channel.

The most important result of the new design with respect to gradient generation, is the small discrepancy in buffer composition between the electrode and separation channels from top to bottom. As already mentioned, there is an ~16-fold linear velocity difference between the electrode and separation channels. With the new design, both channels are fed by the same buffer source. Therefore during the application of a gradient, the composition of the buffer when split between the high and low linear velocity channels is identical. However, because of the different linear velocities within the channels, the gradient reaches the outlet of the electrode channel ~16 times faster than in the separation channel. As a result, a concentration mismatch (CM) is created between the channels and is a function of the flow rate and the gradient speed:

$$\%\mathrm{CM}=\frac{L\left(\frac{1}{v_{\mathrm{SC}}}-\frac{1}{v_{\mathrm{EC}}}\right)}{t_{\mathrm{g}}}\times 100\% \tag{6}$$

where t_g is the gradient time, L is the length of the channels, and v_{EC} and v_{SC} are the linear velocities in the electrode and separation channels, respectively. Thus at a standard flow rate of 0.5 mL/ min where linear velocities in the electrode and separation channels are 2.6 cm/s and 0.16 cm/s, respectively, the maximum temporal difference over the 2.5 cm length of the channel is ~15 s. In terms of the 5 min gradient run during the experiments described herein, this corresponds to a modest 5% difference in buffer composition between the electrode and separation channel at the outlet of the device.

Gradient Characterization

Fluorescein gradients were applied to the new μ-FFE device to characterize the profile of the gradient. A region near the inlet of the separation channel was imaged as gradients with different rates of change were applied (see Figure 3). The slopes of the 5 and 10 min gradients are quite linear. Faster gradients are ideal because they will minimize the time required to test a range of separation conditions. Longer gradients were less linear, especially at the beginning and end of the gradient. This is consistent with the diffusion expected to take place as the gradient moves from the mixing cross to the inlet of the μ-FFE device. Gradient times shorter

than 5 min were avoided because the concentration mismatch between the electrode and separation channel increases dramatically as the gradient time decreases (see eq 6).

HP-β-CD Gradients

Separations of NBD–Gly, NBD–L-Ser, and NBD–PEA were performed while applying a 0–50 mM HP-β-CD gradient over 5 min. Cyclodextrins are commonly used in CE separations to improve resolution of comigrating peaks, particularly enantiomers.[27–29] Analyte mobilities are shifted as analytes bind the hydrophobic cavity of the cyclodextrin.[28] Cyclodextrins have previously been used to optimize the separation of NBD-labeled amino acids, so this makes for an excellent proof of concept experiment.[30]

The effect of the HP-β-CD gradient on the μ-FFE separation is shown in Figure 4. The plot clearly illustrates some qualitative aspects of the separation of these three NBD-labeled primary amines. (1) There are several ranges of HP-β-CD concentration where the analytes are completely resolved. At the start of the gradient, NBD–L-Ser is unresolved from NBD–PEA but is quickly resolved with a small increase in HP-β-CD concentration. As the increasing HP-β-CD concentration continues to shift the mobility of NBD–L-Ser, it again becomes unresolved, now with NBD– Gly at ~3 mM HP-β-CD. Finally at all higher HP-β-CD concentrations, the three analytes are completely resolved. (2) The relative association of each analyte with HP-β-CD can be easily compared. The mobility shift, illustrated as a change in position of the analytes, closely resembles a binding curve. For the NBD–L-Ser peak, which passes through both other peaks, there is obviously a much stronger affinity indicated by the slope and curvature of the mobility shift.

Figure 4B is a plot of the average peak position from three successive gradient runs at the corresponding HP-β-CD concentrations. The standard error for three experiments (dotted lines) indicates that the gradient can be applied with a high level of reproducibility. What is most surprising is the very small error for the NBD–L-Ser peak considering it has such a large mobility shift, further indicating the precision of the method.

Comparison with CE

The μ-FFE separations of the three NBD-labeled primary amines were compared with CE separations performed under the same buffer conditions. The mechanism of separation is identical in both cases, and similar results were expected. The results of this comparison are highlighted in Figure 5. The left panel (Figure 5A) shows representative μ-FFE separations recorded during the application of the HP-β-CD gradient. The analytes are detected as fluorescent spots as the streams cross the Ar^+ laser beam focused in a line across the separation channel. The four concentrations shown depict the four possible cases of analyte separation. Figure 5B shows the linescans of the same data giving results analogous to electropherograms, allowing a straightforward comparison with the CE electropherograms shown in Figure 5C. The profiles of the electropherograms from both techniques are qualitatively similar. Peak efficiency is obviously higher in the CE separations, but the migration order observed in the electropherograms at different HP-β-CD concentrations are remarkably similar. This is important because it suggests that data obtained using gradient μ-FFE may be predictive of CE and therefore useful in optimizing CE separation conditions.

Two key differences between the gradient μ-FFE and CE experiments are the time it takes to collect the data and the amount of data that is collected. In the CE experiments, 15 separations were performed to sample across the range of HP-β-CD concentrations. Even with relatively short separation times of 2.5 min, it took over 4 h to perform these experiments. In contrast, the gradient μ-FFE experiment provided nearly continuous coverage across the HP-β-CD gradient in 5 min. The only limitation arises from the sampling rate of the CCD camera when

acquiring fluorescence images. Images were acquired every 5 s over the 5 min gradient generating 60 separate linescans. This corresponds to four times as much data in 50-fold less time. The difference in HP-β-CD concentration between linescans was less than 1 mM. While not necessary for the current experiment, the sampling rate could have easily been increased to 1 Hz, generating 0.17 mM steps. The advantage of the continuous μ-FFE approach is that data is collected for every possible buffer composition across the range of the gradient, eliminating the need to interpolate between discrete experiments, as is common in CE experiments.

Equilibrium Constant Measurements

Mobility data acquired across a range of HP-β-CD concentrations using gradient μ-FFE and CE were fit to eq 5 to make a more quantitative comparison between the techniques. The 60 points recorded for NBD–L-Ser during the 5 min μ-FFE gradient are plotted in Figure 6A (red circles). The shape of the curve is typical for 1:1 binding. Data recorded using CE are also plotted in Figure 6A (blue diamonds). The curves are remarkably similar. Table 1 compares the dissociation constants and changes in mobility estimated using the two data sets. The dissociation constants estimated for the NBD–L-Ser–HP-β-CD complex are statistically indistinguishable. The range of the mobility change is also nearly identical. Again, a key difference in the techniques is that gradient μ-FFE was able to obtain 60 points in 5 min while the CE experiment required 4 h to obtain 15 points. An additional difference between the techniques was the reproducibility of the observed data. In CE experiments performed over long periods of time, mobility data must be corrected to account for variations in the electroosmotic flow (EOF). In the present example, EOF changed by 60% over the 4 h required to collect the CE data, much more than would be predicted by changes in viscosity alone. This correction was not necessary when using the μ-FFE-based method, most likely because all of the data could be recorded in a short period of time, giving less opportunity for drift in the EOF to occur. Uncorrected data was even reproducible in multiple subsequent gradient μ-FFE experiments, as shown in Figure 4B.

Parts B and C of Figure 6 show the mobility data recorded using μ-FFE and CE for NBD–Gly and NBD–PEA, respectively. Again, the data in all cases is described very well using eq 5. Whereas the curves recorded using μ-FFE and CE for NBD–Gly and NBD–PEA are similar, upon closer examination they are distinctly different. The rate of curvature is higher in the μ-FFE data than the CE data giving rise to lower estimates for the dissociation constants (see Table 1). The range of the observed mobility change is also lower in the μ-FFE data. There are a number of possible causes for this discrepancy. The concentration mismatch between the separation channel and the electrode channels also gives rise to a viscosity mismatch, which could affect the flow profile through the device. According to eqs 4 and 5, the maximum viscosity difference between the electrode and separation channels observed during the application of a 5 min gradient would be 1.6%. It is unlikely that such a small viscosity difference would give rise to the differences observed in Figure 6B,C. Additionally a change in the flow profile would be expected to affect the mobility of NBD–L-Ser more than NBD–Gly and NBD–PEA because this analyte travels closer to the edge of the separation channel at higher HP-β-CD concentrations. Another possibility is a change in EOF over the 5 min application of the gradient that is not accounted for by the viscosity correction factor. Whereas this is possible, it does not explain why the μ-*FFE* and CE data for NBD–L-Ser match so well. The most likely explanation is variability in the time course of the applied gradient. The data shown in Figure 3 was used to predict the time course of the gradient and calculate the HP-β-CD concentration for every μ-FFE separation recorded. If the timing or shape of this gradient changes, the concentrations plotted on the *x*-axis of Figure 6 will be incorrect. This will be more of a problem at the beginning and end of the experiment, where the gradient is least linear. The data for NBD–L-Ser has plateaued well before the end of the gradient, suggesting that any

error in [HP-β-CD] at this point will have minimal effect on the curve. The mobilities for NBD–Gly and NBD–PEA continue to vary across the gradient. Errors in [HP-β-CD] would therefore have a much more significant effect on these curves. This suggests that gradient μ-FFE would benefit from a more sophisticated method for generating the buffer gradient such as a μHPLC pump. Alternatively, the range of the gradient should extend beyond the range where significant changes in mobility are expected to be observed.

Conclusions

We have demonstrated the application of gradient μ-FFE for fast electrophoretic separation optimization and equilibrium constant determination. The continuous nature of μ-*FFE* separations allows data to be recorded continuously as buffer conditions are varied in the device. In comparison to discrete separation techniques such as CE, gradient μ-FFE allows many more data points to be recorded in dramatically less time. This allows complete coverage across a range in buffer conditions. Beyond the obvious throughput advantages, collecting data at every set of conditions makes interpolation from limited data sets unnecessary. Finding the optimum separation conditions is as simple as scanning through the data set. More data points also improves the precision of equilibrium constant estimates without requiring a significant increase in the time required for data collection. Although HP-β-CD was used as the buffer additive in these proof of concept experiments, gradients of other buffer conditions such as pH, ionic strength, etc. could easily be introduced into the μ-FFE device for optimization of these parameters.

Acknowledgments

Funding for this research was provided by the National Institutes of Health (Grants GM 063533 and NS 043304). Computations were made possible by a resource allocation from the Scientific Development and Visualization Laboratory of the University of Minnesota Supercomputing Institute.

References

1. Fonslow BR, Barocas VH, Bowser MT. Anal Chem 2006;78:5369–5374. [PubMed: 16878871]
2. Raymond DE, Manz A, Widmer HM. Anal Chem 1994;66:2858–2865.
3. Raymond DE, Manz A, Widmer HM. Anal Chem 1996;68:2515–2522.
4. Fonslow BR, Bowser MT. Anal Chem 2005;77:5706–5710. [PubMed: 16131085]
5. Zhang CX, Manz A. Anal Chem 2003;75:5759–5766. [PubMed: 14588015]
6. Kohlheyer D, Besselink GAJ, Schlautmann S, Schasfoort RBM. Lab Chip 2006;6:374–380. [PubMed: 16511620]
7. Kobayashi H, Shimamura K, Akaida T, Sakano K, Tajima N, Funazaki J, Suzuki H, Shinohara E. J Chromatogr, A 2003;990:169–178. [PubMed: 12685595]
8. Graham JM, Wilson RBJ, Patel K. Methodol Surv Biochem Anal 1987;17:143–152.
9. Heidrich HG, Hannig K. Methods Enzymol 1989;171:513–531. [PubMed: 2687642]
10. Hoffstetter-Kuhn S, Kuhn R, Wagner H. Electrophoresis 1990;11:304–309. [PubMed: 2187696]
11. Hoffstetter-Kuhn S, Wagner H. Electrophoresis 1990;11:451–456. [PubMed: 2203646]
12. Hoffstetter-Kuhn S, Wagner H. Electrophoresis 1990;11:457–462. [PubMed: 2203647]
13. Kessler R, Manz HJ. Electrophoresis 1990;11:979–980. [PubMed: 2079047]
14. Poggel M, Melin T. Electrophoresis 2001;22:1008–1015. [PubMed: 11358121]
15. Wang Y, Hancock WS, Weber G, Eckerskorn C, Palmer-Toy D. J Chromatogr, A 2004;1053:269–278. [PubMed: 15543993]
16. Zischka H, Weber G, Weber PJA, Posch A, Braun RJ, Buehringer D, Schneider U, Nissum M, Meitinger T, Ueffing M, Eckerskorn C. Proteomics 2003;3:906–916. [PubMed: 12833514]
17. Zuo X, Lee K, Speicher DW. Proteome Anal 2004:93–118.

18. Shinohara E, Tajima N, Suzuki H, Funazaki J. Anal Sci 2001;17:i441–443.
19. Pereira de Jesus D, Blanes L, do Lago CL. Electrophoresis 2006;27:4935–4942. [PubMed: 17161008]
20. Kohlheyer D, Eijkel JCT, Schlautmann S, van den Berg A, Schasfoort RBM. Anal Chem 2007;79:8190–8198. [PubMed: 17902700]
21. Janasek D, Schilling M, Manz A, Franzke J. Lab Chip 2006;6:710–713. [PubMed: 16738720]
22. Fonslow BR, Bowser MT. Anal Chem 2006;78:8236–8244. [PubMed: 17165812]
23. Weinberger, R. Practical Capillary Electrophoresis. Vol. 2nd. Academic Press; San Diego, CA: 2000.
24. Gilges M, Kleemiss MH, Schomburg G. Anal Chem 1994;66:2038–2046.
25. Shackman JG, Watson CJ, Kennedy RT. J Chromatogr, A 2004;1040:273–282. [PubMed: 15230534]
26. Peng X, Bowser MT, Britz-McKibbin P, Bebault GM, Morris JR, Chen DDY. Electrophoresis 1997;18:706–716. [PubMed: 9194595]
27. Lelievre F, Gareil P, Bahaddi Y, Galons H. Anal Chem 1997;69:393–401.
28. Terabe S, Ozaki H, Otsuka K, Ando T. J Chromatogr 1985;332:211–217.
29. Wren SAC, Rowe RC. J Chromatogr 1992;603:235–241.
30. Ciriacks Klinker C, Bowser MT. Anal Chem 2007;79:8747–8754. [PubMed: 17929877]

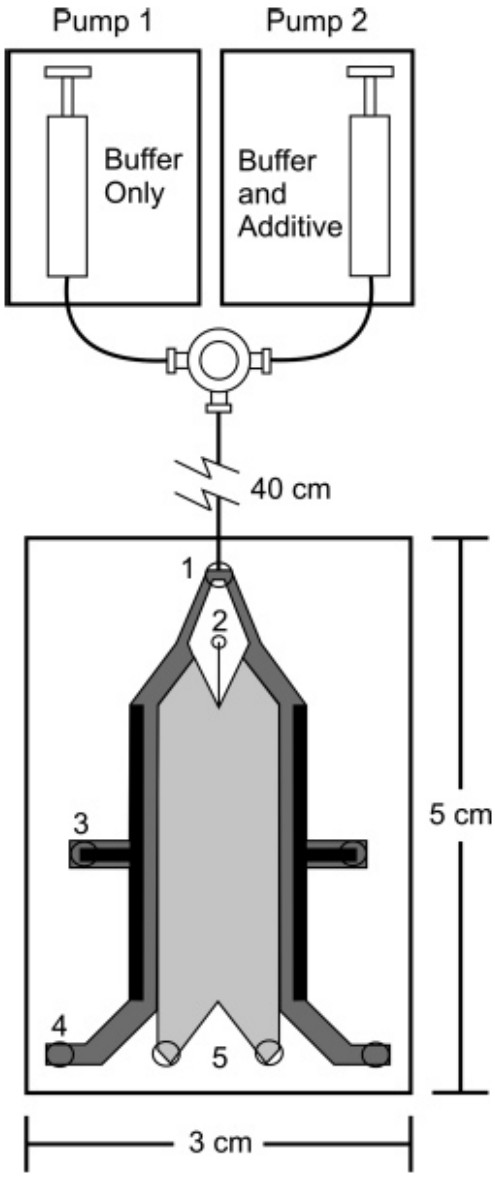

Figure 1.
Schematic of the μ-FFE pumping setup used for generating a buffer additive gradient. Pump 1 and 2 were controlled using LabView to ramp the flow rates to create the gradient while keeping the flow rate constant. Mixed buffer solutions were pumped into the chip buffer inlet (1) from the mixing tee. Sample was pumped in at the chip sample inlet (2). The mixed buffer flowed through the deeper electrode channels (dark gray regions) and shallow separation channel (light gray regions). Buffer exited the chip at the two electrode channel outlets (4) and the two separation channel outlets (5). Voltage was applied to electrodes (black regions) via the electrode access holes (3). All channels were sealed by bonding two glass wafers together (white regions).

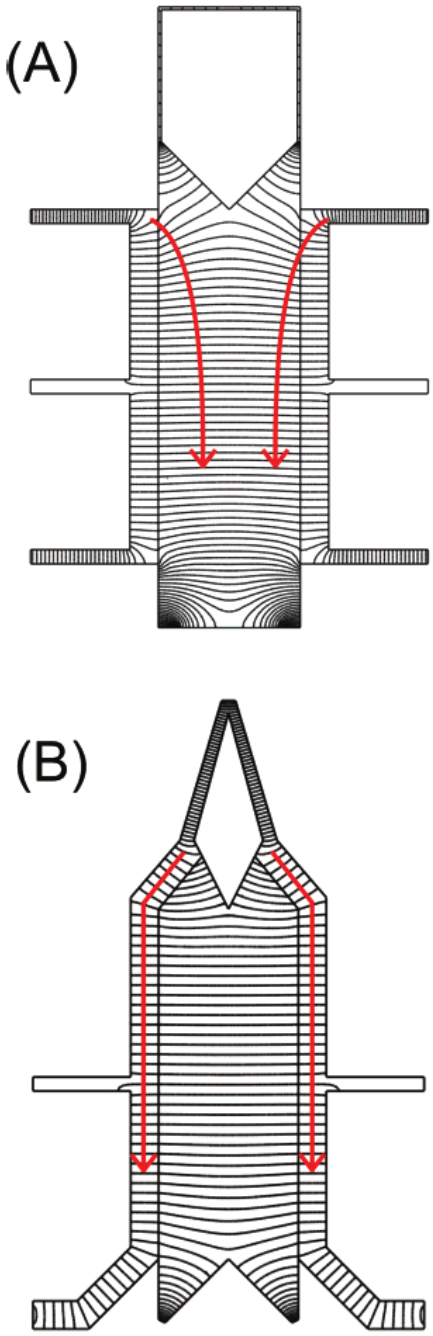

Figure 2.
Comparison of the equal pressure lines in an (A) earlier[1] and (B) new two-depth μ-FFE design. Contour plots were generated using COMSOL modeling. Red arrows were drawn perpendicularly to the equal pressure lines to illustrate flow paths in the electrode channels.

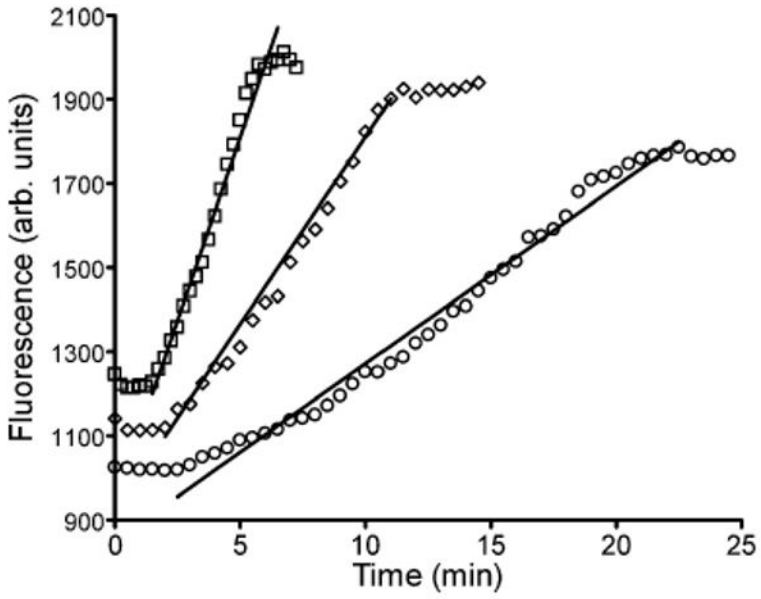

Figure 3.
Measurement of fluorescein concentration gradients in the μ-FFE separation channel. Gradients were run over periods of 5 (□), 10 (◊), and 20 (○) min.

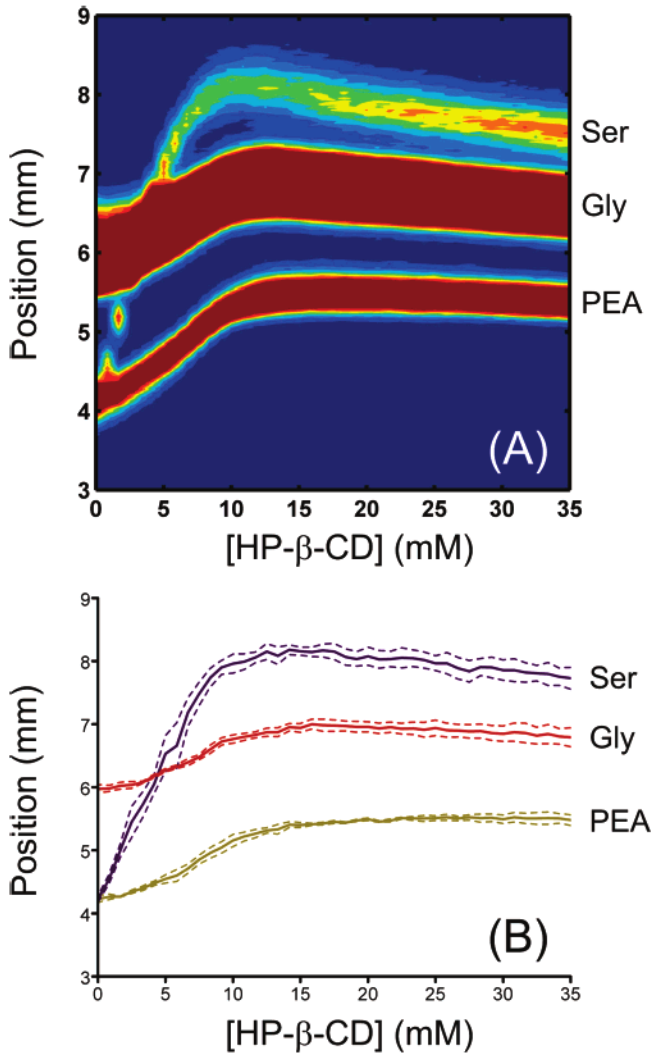

Figure 4.
(A) Contour plot illustrating μ-FFE separations of NBD–L-Ser, NBD–Gly, and NBD–PEA recorded during a 5 min HP-β-CD gradient. The contour plot was made up of successive linescans acquired every 5 s (42 total) corresponding to 0.8 mM HP-β-CD steps. (B) Average peak position of NBD–L-Ser (blue), NBD–Gly (red), and NBD–PEA (green) recorded in three successive 5 min HP-β-CD gradients. Dashed lines bound the standard error of the mean. The cathode is at the top of the plots, and the anode is at the bottom.

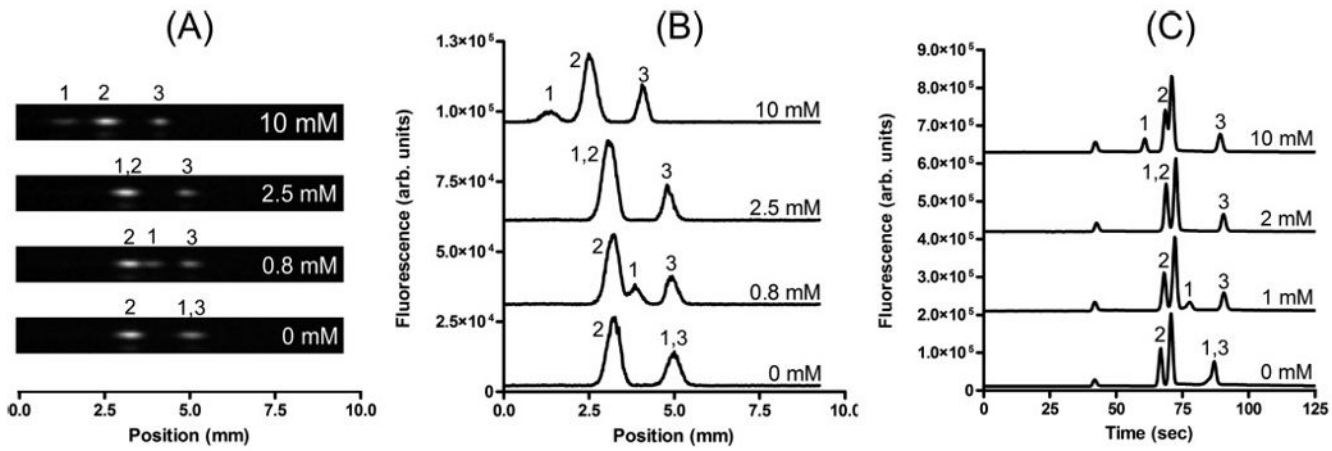

Figure 5.

Comparison of (A) μ-FFE images, (B) μ-FFE linescans, and (C) CE electropherograms for NBD–L-Ser (1), NBD–Gly (2), and NBD–PEA (3) measured under similar HP-β-CD concentrations. In parts A and B, the cathode is on the left and the anode is on the right.

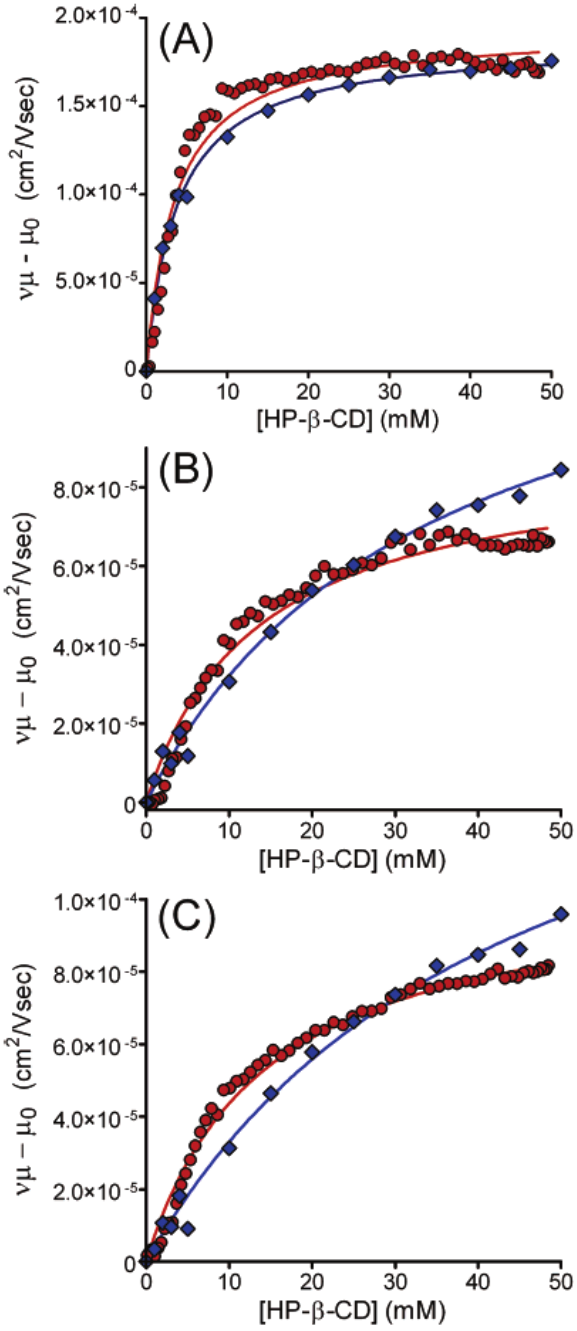

Figure 6.

Comparison of the effect of HP-*β*-CD concentration on mobilities observed for (A) NBD–L-Ser, (B) NBD–Gly, and (C) NBD–PEA using *μ*-FFE (red circles) and CE (blue diamonds). Data were fit to an equation describing a 1:1 analyte–additive equilibrium (eq 5) to estimate dissociation constants and changes in mobility.

Table 1

Dissociation Constants (K_D) and Change in Mobility ($\mu_{AC} - \mu_0$) of NBD-Labeled Primary Amine–HP-β-CD Complexes Estimated Using μ-FFE and CE[a]

	K_D (mM)			$\mu_{AC} - \mu_0$ (10^{-5} cm^2/V s)		
analyte	**μ-FFE**	**CE**	***p***	**μ-FFE**	**CE**	***p***
NBD–L-Ser	3.5 ± 0.5	3.8 ± 0.3	0.64	19.3 ± 0.6	18.6 ± 0.4	0.25
NBD–Gly	13 ± 2	34 ± 10	1.6×10^{-8}	8.9 ± 0.5	14 ± 2	3.5×10^{-10}
NBD–PEA	14 ± 1	44 ± 15	3.1×10^{-11}	10.6 ± 0.4	18 ± 2	1.18×10^{-11}

[a]Error limits are the 95% confidence intervals.